

28. Kunte, K., *Butterflies of Peninsular India* (ed. Gadgil, M.), Orient Longman, Hyderabad, 2000.
29. Voogd, H., *Multi-criteria Evaluation for Urban and Regional Planning*, Pion Ltd, London, 1983.
30. Duckworth, J. W. and Hedges, S., *Tracking Tigers*. Report, WWF, Indo-China Programme, Hanoi, 1998.

**ACKNOWLEDGEMENTS.** This work was supported by the John, D. and Catherine T. MacArthur Foundation, USA. We would also like to thank the Wildlife Preservation Trust International, USA (now the Wildlife Trust) for actively supporting our research. We thank the Forest Departments of Karnataka, Kerala and Tamil Nadu for permission to carry out field surveys in the elephant reserves and providing logistic support and information when needed. Joshua David collected and collated a subset of the data that were eventually incorporated in the database. Kumaran Raju provided additional GIS support.

Received 6 November 2001; revised accepted 31 January 2002

## Identification and usage of multiples in crustal seismics – An application in the Bengal Basin, India

A. S. S. R. S. Prasad, D. Sarkar and P. R. Reddy\*

National Geophysical Research Institute, Hyderabad 500 007, India

**Multiple seismic phases associated with deeper horizons have been observed in long-range seismic refraction sections. These have been successfully distinguished from the primary events and utilized to build crustal velocity–depth section along Gopali–Port Canning profile, Bengal Basin.**

PHASE identification is the basic component of seismic data processing. The phase may correspond to primary events like refraction, reflection, diffraction and converted wave. In addition, multiples of various kinds are observed in some cases depending on the geological setting of the region. These phases in favourable circumstances can be identified and distinguished from the primary using the difference in their arrival times. These multiples (conventionally viewed as ‘noise’) have been utilized as ‘seismic signals’ to build up velocity–depth models<sup>1–3</sup>.

Crustal velocity–depth section<sup>4</sup> was built along a profile in West Bengal Basin (Figure 1; first arrival refraction and later arrival wide-angle reflections) using only primary phases. Crustal section along this profile,

viz. Gopali–Port Canning provided velocity–depth details of the sedimentary column, basement and sub-basement crust. Subsequently, an additional layer has been introduced<sup>5</sup> at the lower crustal level utilizing only primary phases. As the record sections of Gopali–Port Canning contain significantly high amplitude multiples, 2D velocity–depth sections down to the basement have been built<sup>2,3</sup> by using free surface multiple diving waves and multiple reflections. These velocity–depth sections, generated by using multiples were better constrained to claim higher accuracy. These sections have brought into focus the finer variations in the velocity gradients in different shallower layers, which otherwise could not have been obtained from the processing of primary phases alone.

The multiples associated with deeper layers have neither been identified nor utilized earlier. Refraction seismograms of Gopali–Port Canning profile are seen to have several strong phases even at a distance of 80 to 130 km away from the source. These phases are seen intermixing with the primary phases. Seismograms of all the shot points contain the phases that are identified as peg-leg multiples<sup>6–8</sup> and reflected refractions<sup>1,9,10</sup>. These are the multiple events reflected from deeper boundaries (basement, sub-basement and the Moho). In the subsequent exercise, modelling of primary events along with the multiples has been carried out. These newly identified phases have thus been utilized to test and modify the crustal velocity model derived earlier<sup>5</sup>. In the process nearly all the prominent phases, which were present in the observed seismograms but remained unexplained have been synthetically reproduced, for increasing confidence in the constructed model.

Multiples are reflections that have undergone more than one bounce. It means that the wave gets reflected by the same or another reflector one or more times and returns to the surface to be recorded by the geophones<sup>11</sup>.

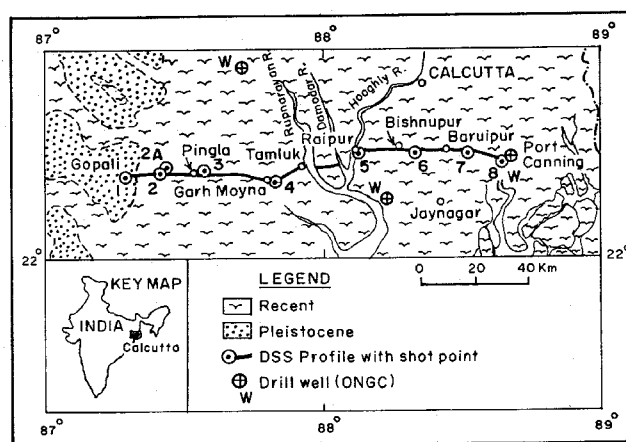


**Figure 1.** Location map of Gopali–Port Canning profile in West Bengal Basin on the geological map of the region.

\*For correspondence.

The geophones thus receive signals more than once from the same seismic reflector. The first multiple path is approximately twice the length of the primary ray path. If the travel time for the first multiple is  $t$ , the travel time for the second multiple will be approximately  $2t$ . The first multiple will thus appear on the seismic section as a reflection at a time  $t$  below the primary event<sup>11</sup> (as shown in the Figure 2a); the second multiple will appear at a time  $2t$  and so on.

Multiples are classified into free surface multiples<sup>1</sup> (multiple diving and multiple reflections), long- and short-path multiples and ghosts<sup>11</sup>. Multiple diving waves are generated when the diving waves get reflected at the free surface of the earth one or more times. These arrivals appear in arcuate shapes on a travel time plot with their curvature concave downwards. The multiple diving waves are produced with strong amplitude character, if high velocity gradients are present in the sedimentary layers. The curvature of the multiple reflection travel is concave upwards. Peg-leg multiples are caused by an extra bounce between two reflectors. Long-path multiples appear as separate reflections because the travel path is large compared to the primary reflections. In a condition as like in Figure 2b, the short-path multiples arrive at the surface slightly after the primary reflection because the bed is very thin. They interfere with the primary reflections. The short-path multiples appear as separate events if the layer is dipping or thick. Ghosts are short-path multiples, common to both land and marine seismic sections. These occur when seismic energy that initially travelled upward from the source, is reflected downward from the surface or base of the weathering zone. They closely

follow the same travel path of the main pulse in the downward direction (Figure 2b). They reach the surface almost as close as the primary reflection.

Two-dimensional forward ray-tracing technique Rayamp-PC (ref. 12) is an effective algorithm for computing synthetic seismograms in laterally inhomogeneous media. The method based on zero-order asymptotic ray theory (ART), which has high frequency approximation, corresponds to the geometrical optics solution. It is primarily intended for use in refraction and reflection studies, and provides an economical means of seismic modelling. A 2D velocity-depth model is divided into a number of boundaries. Each has a velocity and a gradient assigned to it. Each boundary contains constant seismic parameters. First-order interfaces are represented by an arbitrary number of dipping linear segments. Amplitudes are determined by generating spreading of spherical wave fronts and energy-partitioning at interfaces.

To generate primary refractions, reflections, and multiple events and the corresponding seismograms, we used Rayamp-PC (ref. 12) program. The ray paths of multiple phases used are shown in Figure 3. This program offers the possibility of investigating the individual elementary waves. This has proven to be very useful in the interpretation of the peg-leg multiples originating from the deeper horizons. Since the final model largely depends on a correct treatment of amplitudes<sup>2</sup> during modelling, this aspect has been taken into consideration both in identification, generation and usage of peg-leg multiples and reflected refractions. In processing the data care has been taken in adjusting interfaces and the velocity contrasts until we arrived at satisfactory matches between the observed and synthetic record sections for all shot points. As seen from Figures 4 and 5, the ray method, though approximate in modelling, has produced synthetic record sections well matched with the observed ones.

The record sections observed for different shot points and the corresponding synthetic seismograms for the final model developed are strikingly similar. SP 7 sections (Figure 4a) are shown as an example. Travel-time curves of SP 7 (Figure 4a, b) for various phases are marked by  $P$ -refraction and reflection phases, long-path multiples ( $P^{2.7}P^{6.8}$ , etc.), short-path (peg-leg) multiples ( $P^{8.1}P^{2.7}$  and  $P^{7.5}P^{2.7}$ , etc.) and reflected refractions ( $P_{6.0}P^{2.7}$ , etc.). The primary wide angle reflection phases from LVL (velocity of 5.7 km/s), upper (velocity 6.4 km/s), middle (velocity 6.8 km/s), and lower crust (velocity 7.5 km/s), and the Moho (velocity 8.1 km/s) are present in the seismogram. A close observation of the primary and multiple events (observed) and the generated synthetic seismograms clearly indicates a one-to-one correspondence, which obviously justifies the adopted methodology.

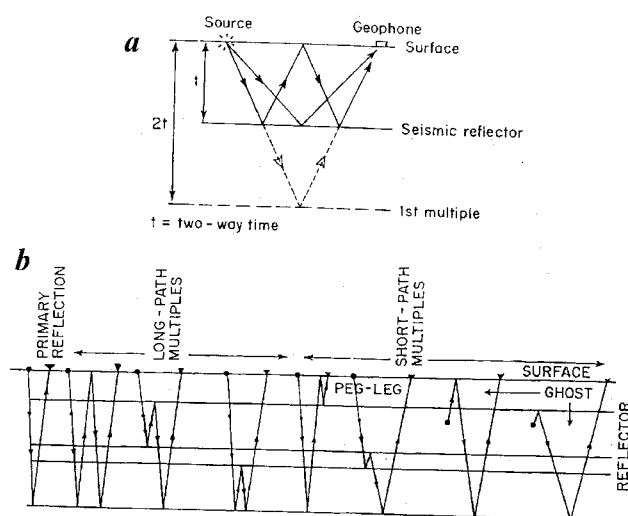


**Figure 2.** Schematic diagram of (a) primary reflection and simple multiple; and (b) common types of multiple reflection (courtesy: Badley<sup>11</sup>).

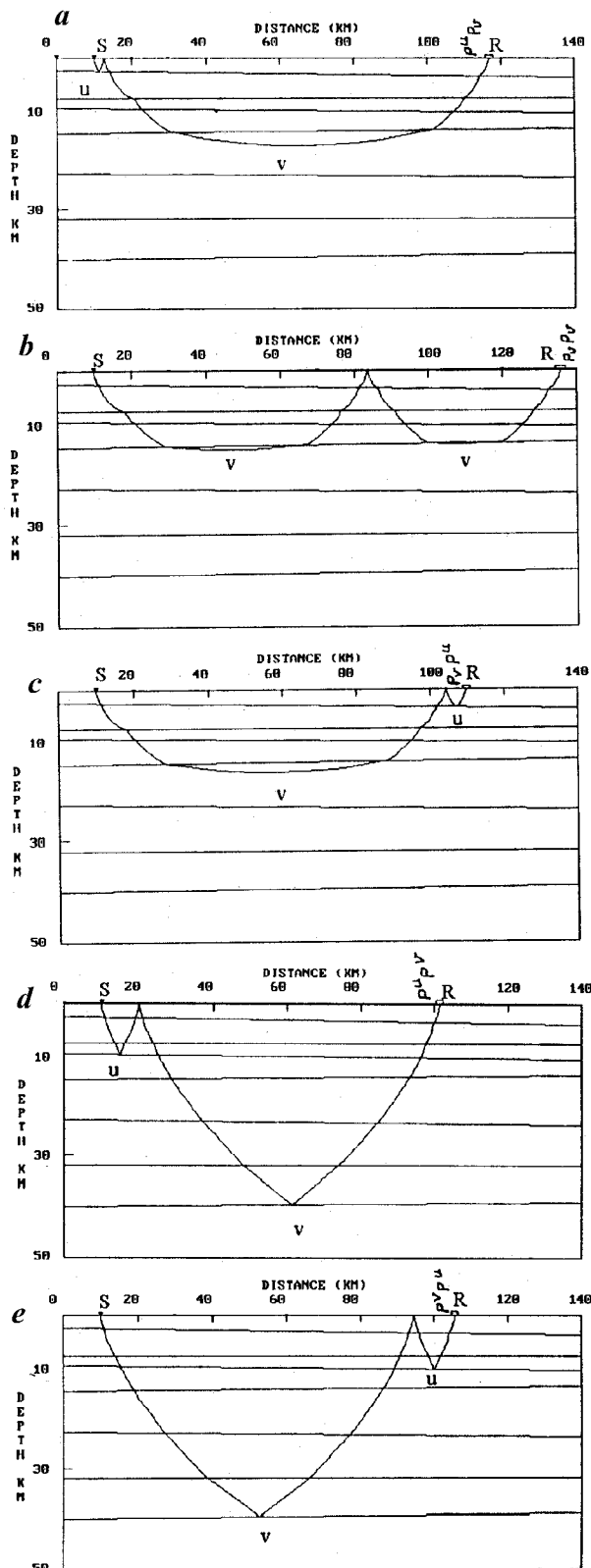


**Figure 3.** Schematic ray diagram showing rays for reflected refractions (*a-c*), long-path multiples (*d*) and short-path (peg-leg) multiples (*e*), where  $v$  and  $u$  correspond to the velocity (km/s) of the layers.  $S$  and  $R$  are the source and receiver positions, respectively.  $P_v$  represents a refraction through the final layer with velocity  $v$ ,  $P^v$ ,  $P^u$  represent reflections from the top of the layer with velocity  $v$  and  $u$ , respectively.

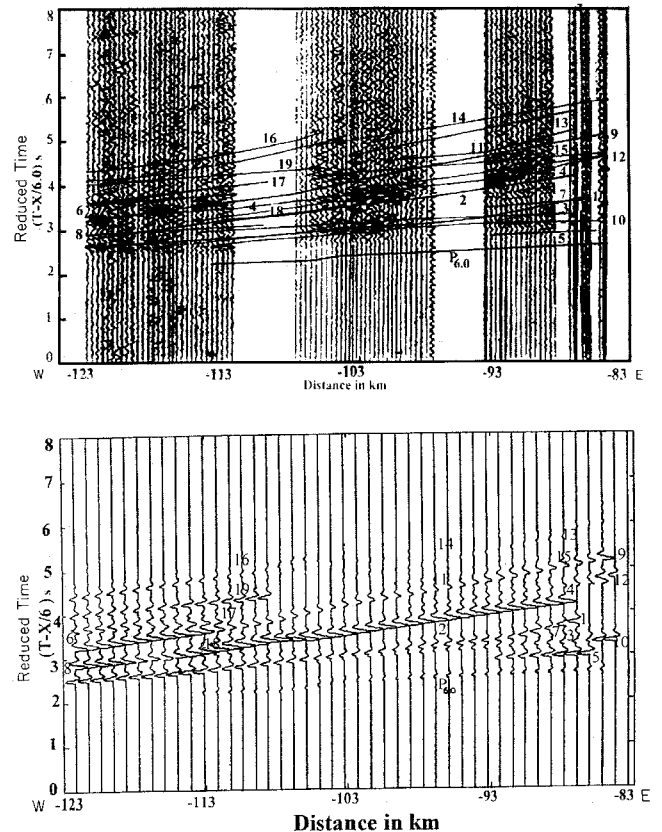


**Figure 4.** Record sections of (*a*) observed and (*b*) synthetic seismograms for SP 7. Travel-time curve phases, are marked by  $P$  refractions and wide-angle reflection phases from upper crust, mid crust, lower crust and the Moho (indicated with the numbers as 5 ( $P^{6.4}$  or  $P^{6.45}$ ), 1 ( $P^{6.8}$  or  $P^{6.85}$ ), 2 ( $P^{7.5}$ ) and 9 ( $P^{8.1}$ ), respectively), boundaries and long-path multiples from mid-crust (4 ( $P^{2.7}P^{6.8}$ )), the Moho (14 ( $P^{2.7}P^{8.1}$ )), short-path (peg-leg) multiples from upper crust (7 ( $P^{6.4}P^{2.7}$ )), mid-crust (6 ( $P^{6.8}P^{5.5}$ ), 8 ( $P^{6.8}P^{2.7}$ ), 11 ( $P^{6.8}P^{3.8}$ ), lower crust (19 ( $P^{7.5}P^{5.5}$ )) and the Moho (13 ( $P^{8.1}P^{2.7}$ ) and 17 ( $P^{8.1}P^{2.7}$ ), 16 ( $P^{8.1}P^{5.5}$ ) and reflected refractions from basement (3 ( $P^{2.7}P_{6.0}$ ), 10 ( $P_{6.0}P^{2.7}$ ), 12 ( $P_{6.0}P^{5.5}$ ), 15 ( $P_{6.0}P_{6.0}$ ) and 18 ( $P_{6.0}P^{5.5}$ ) of the primary phases for the model in Figure 6. For naming the phases the norm explained in case of Figure 3 has been followed.

As detailed above, multiples are generated when specific compositional and structural environments are present in the sub-surface geological formations. In the Bengal Basin, favourable geological conditions exist for the generation of peg-leg multiples and reflected refractions. These multiples can be identified and segregated from the primary events mainly due to differences in the arrival time (at a certain source-receiver distance). An example is cited below to give a clear picture. Figure 4*a* and *b* contains both the primary and multiple events. When these are critically studied, it is noticed that the primary event belonging to mid-crustal layer is different in character from the multiple event in the following way:

Figure 4*a* and *b* contains both the primary and multiple events. The primary reflection ( $P^{6.8}$ ) from the mid-

crustal layer is indicated by the numeral 1. This is seen to have arrived at a time of 3.05 s to 2.65 s in the reduced travel time<sup>13</sup>. Normally the peg-leg multiples from deeper layers depend on the velocity, thickness, dip and structure of the shallow layers. If the thickness of top layer, which is near the surface is very thin, then the multiples will arrive soon after the primary reflections. But in the case of a 2D structure, the long-path and short-path (peg-leg) multiples that are generated from deeper layers will have different travel paths compared to the primary. The long-path and short-path (peg-leg) multiples, which are generated from the horizontal layers have identical travel distance curves and appear as one event although they follow different ray-paths.

The present model which is utilized to produce multiples has a complex structure. The generated long-path and short-path (peg-leg) multiples have different travel time because of the dipping effect. The long-path

multiple generated from the mid-crustal layer is indicated by numeral 4 ( $P^{2.7}P^{6.8}$ ). The time of its arrival is clearly different from the primary event arrival (time 4.31 s at 85 km and 3.38 s at 115 km distance from SP 7 compared to time 3.68 s at 85 km and 2.81 s at 115 km for the primary event). This is vividly depicted as a separate event. The short-path (peg-leg) multiple, indicated by numeral 8 ( $P^{6.8}P^{2.7}$ ), has travelled in a different path. It appears as a separate event, but near the primary event (for time 3.10 s at 110 km and 2.93 s at 123 km distance compared to time 2.96 s at 110 km and 2.75 s at 123 km for the primary event), because the thickness of the particular layer is less.

Similar analysis has been done for all primary events and corresponding multiples generated from basement, LVL, lower, middle and upper crust; and the Moho, as shown in the Figures 4 and 5 for SP7 and SP2, respectively.

This paper mainly deals with the multiple events, which appeared at a long range ~80–130 km from the shot-point. The identified multiple events are generated from deeper layers. The multiple reflections from the shallow layers appear near distances from the source. So in the record sections these events are not present. Multiple reflections are also generated along with the primary events and long and short-path multiples. Normally the time taken by multiple reflections from deeper layers to reach the surface is more than 8 s (reduced time). But the available data are up to 8 s (reduced time) only, the source of these multiple reflections is missing (Figures 4a and 5a). To produce ghost reflections, the source should have some depth. In this field study, the source is located very near the surface, so the ghost reflections are not generated.

*A priori* information helps in constraining a better model. As the objective of the present study is identifying, distinguishing and utilizing the multiples from

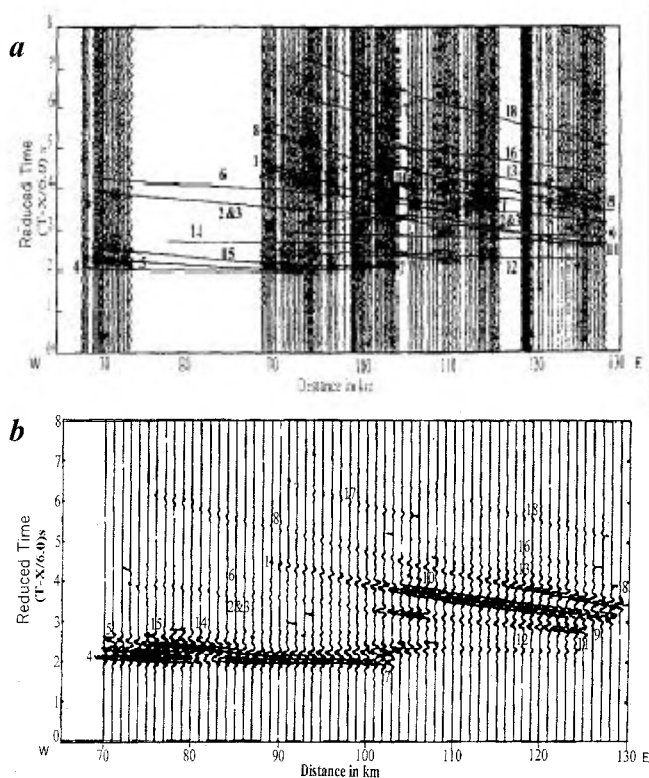


**Figure 5.** Record sections of (a) observed and (b) synthetic seismograms for SP 2. Travel-time curve phases are marked by  $P$  refractions (4 ( $P_{6.0}$ )) and wide-angle reflections phases from LVL, upper crust, mid crust, lower crust and the Moho (indicated with the numbers as 5 ( $P^{5.6}$ ), 7 ( $P^{6.4}$  or  $P^{6.45}$ ), 2 ( $P^{6.8}$  or  $P^{6.85}$ ) and 3 ( $P^{6.8}$  or  $P^{6.85}$ ), 1 ( $P^{7.5}$ ) and 8 ( $P^{8.1}$ ) respectively), boundaries and long-path multiples from LVL (15 ( $P^{2.7}P^{5.6}$ )), upper crust (14 ( $P^{2.7}P^{6.4}$ )) and mid-crust (6 ( $P^{2.7}P^{6.8}$ )) and short-path (peg-leg) multiples from upper crust (9 ( $P^{6.4}P^{2.7}$ )), mid crust (10 ( $P^{6.8}P^{2.7}$ ), 16 ( $P^{6.8}P^{3.8}$ ), lower crust (13 ( $P^{7.5}P^{2.7}$ ), 17 ( $P^{7.5}P^{3.8}$ )) and the Moho (18 ( $P^{8.1}P^{3.8}$ )) and reflected refractions from basement (11 ( $P_{6.0}P^{2.7}$ ), 12 ( $P^{2.7}P_{6.0}$ )) of the primary phases for the model Figure 6.

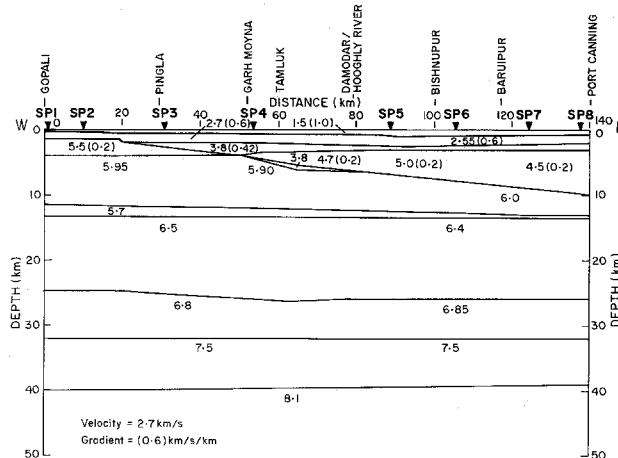


**Figure 6.** Crustal velocity-depth model along Gopali-Port Canning profile as constrained from use of multiple phases.

deeper horizons we have made use of the velocity–depth models<sup>2,3</sup> as initial inputs for the shallower part and the model<sup>5</sup> for the deeper section. The first step led to generation of the multiples using the initial model. After this was carried out through trial and error process we have refined the model in such a way that forward modelling technique has helped in producing both the primary and multiple events that are similar to the observed events on the seismograms of all the shot-points of Gopali–Port Canning profile. Both observed and synthetic seismograms corresponding to the shot-point, SP7 and SP2 are shown (Figures 4 and 5) as they cover both the ends of the Gopali–Port Canning profile and more or less have been used to a major extent in the present study, being long-range mutual shot-points. The wide-angle primary reflections from upper, middle, and lower crust, and the Moho and their long-path and short-path (peg-leg) multiples are visible on the observed seismograms of all shot-points. In addition, we derived the velocity–depth section by using different types of multiples as detailed above (Figure 6), for a better projection of the use of multiples.

This model differs from the earlier<sup>5</sup> model. There is variation in the velocity contrast. The later arrivals that were not considered in the earlier model have also been considered in the present case, with the usage of multiples. This in turn has increased the confidence level of the present model, as the present model has taken into consideration subtle variations in the velocity gradient in the different subsurface layers. There is a slight variation in the thickness (around 500 m) of the LVL compared to the earlier model, with the velocity in the LVL remaining 5.6 km/s. The velocity from the top of the granitic layer to the top of the LVL varies from 5.65 to 6.00 km/s. In the upper crust the velocity varies from 6.35 to 6.6 km/s. The mid-crustal layer (velocity 6.8 to 6.85 km/s) becomes shallower by about 1 km compared to the earlier model. The lower crust having velocity 7.5 km/s is more or less horizontal. The Moho boundary is at 39–40 km depth. The velocity–depth model (Figure 6) explains well, the main features of the observed

record sections. The synthetic seismograms could replicate the observed seismograms in a better way here than those obtained earlier<sup>4</sup> as multiples are also explained in addition to primary refraction and wide-angle reflections.

It is relevant to state that our processing exercise is significant, as identification of multiples associated with deeper horizons (from long-range refraction seismogram), segregating them from primary events and utilizing them to build up velocity–depth models have been carried out, utilizing seismic refraction data generated in India.

The study of different types of multiple events helps in deducing the thickness and velocity of the layers. It has been proved that to construct a better crustal velocity–depth section, one should model not only the primary phases but also their multiples. The use of multiples will provide an opportunity for a re-valuation of existing models of crustal structure.

1. Meissner, R., *Geophys. Prospect.*, 1965, **13**, 617–650.
2. Reddy, P. R. *et al.*, *J. Appl. Geophys.*, 1998, **39**, 109–210.
3. Sarkar, D. *et al.*, *Geophys. J. Int.*, 1995, **121**, 969–974.
4. Kaila, K. L. *et al.*, *Geophys. J. Int.*, 1992, **111**, 45–66.
5. Mall, D. M. *et al.*, *Geophys. Res. Lett.*, 1999, **26**, 2545–2548.
6. Riley, Don, C. and Claerbout, Jon, F., *Geophysics*, 1976, **41**, 592–620.
7. Levin, F. K. and Shah, P. M., *Geophysics*, 1977, **42**, 957–981.
8. Estenez, Raul and Claerbout, Jon, F., *Geophysics*, 1982, **47**, 1255–1272.
9. Day, G. A. and Edwards, G. W. F., *First Break*, 1983, **1**, 14–17.
10. Leutgert, James, H. *et al.*, *Seismol. Res. Lett.*, 1994, **65**, 180–191.
11. Badley, M. E., *Practical Seismic Interpretation*, IHRDC, 1985, pp. 29–70.
12. Rayamp, P. C., Version 2.1, *Geophysics Lab*, McHill University, 1987.
13. Reddy, P. R. *et al.*, *J. Geol. Soc. India*, 1995, **45**, 97–106.

ACKNOWLEDGEMENTS. We are thankful to Dr S. M. Naqvi, Director, NGRI for permission to publish this paper. We also thank Sri M. Shankariah and Sri B. P. S. Rana for preparing the figures.

Received 27 June 2001; revised accepted 8 January 2002